5. Nelson, C. R., Doctorate dissertation, Univ. Michigan, Ann Arbor (1935).
6. McCabe, W. L., and R. P. Stevens, *Chem. Eng. Progr.*, **47**, 168-174 (1951).
7. Hixson, A. W., and K. L. Knox, *Ind. Eng. Chem.*, **43**, 2144-2151 (1951).
8. Bransom, S. H., *Brit. Chem. Eng.*, **5**, 838-844 (1960).
9. Randolph, A. D., and M. A. Larson, *A.I.Ch.E. J.*, **8**, 639-645 (1962).
10. Saeman, W. C., *ibid.*, **2**, 107-112 (1956).
11. Bennett, R. C., *Chem. Eng. Progr.*, **58**, No. 9, 76-80 (1962).
12. Powers, H. E. C., *Intern. Sugar J.*, **50**, 149 (1948).

Manuscript received January 17, 1966; revision received June 13, 1966; paper accepted June 14, 1966.

Stratified Laminar Flow in Ducts of Arbitrary Shape

H. S. YU and E. M. SPARROW

University of Minnesota, Minneapolis, Minnesota

A method of analysis is presented for determining closed-form solutions for two-component stratified laminar flow in horizontal ducts of arbitrary cross section. It is demonstrated that the method is remarkably easy to apply and produces results of high accuracy. As an application, solutions are obtained for stratified flow in a circular tube. The results are compared with various limiting cases and excellent agreement is found to exist. Among the limiting cases, an exact solution was derived by Green's functions for the problem in which the interface between the flow components is situated at the horizontal diametral plane.

Consideration is given to the laminar stratified flow of two immiscible fluids in horizontal ducts of arbitrary cross section. The general area of two-component laminar flows of immiscible fluids has evoked considerable interest in recent years, especially in connection with the pipeline transport of highly viscous liquids. If the component fluids are of different density and if both components experience laminar flow, then a stratified motion (heavier fluid below, lighter fluid above) appears likely. Such motions have been demonstrated experimentally (*1, 2*). In particular, by employing visualization techniques, Charles and Lilleleht (2) have shown that laminar stratified flow with a smooth, ripple-free interface between the components is physically realizable.

This paper is concerned with the analytical treatment of laminar stratified flows in horizontal ducts. A general method of analysis is developed which provides *closed-form* solutions for stratified flows in ducts of arbitrary cross section while taking advantage of universally available computer routines. The method is remarkably easy to apply and, as will be subsequently demonstrated, provides results of high accuracy. Its flexibility is evidenced by the fact that once a computer program has been devised for evaluating the solution for one duct cross section, then the same program is applicable for any cross-sectional shape. These closed-form solutions provide information on local quantities such as the velocity distribution and wall shear as well as for overall quantities such as the flow rate of each component, the pressure drop, and so forth.

The solution method is illustrated by application to the technically interesting case of stratified flow in a horizontal circular tube. Results are obtained for a wide range in the ratio of the viscosities of the component fluids and for a large number of positions of the interface between the stratified layers. For the case in which the interface coincides with the horizontal diametral plane, an *exact* closed-form solution can be derived. This latter solution is employed as a standard against which are compared the results from the general solution method. Other limiting cases are also used in verifying the results of the new solution method.

As noted above, the same computer program employed in obtaining results for the circular tube is applicable, without essential modification, to ducts of any cross-sectional shape. However, no additional duct shapes were considered inasmuch as it is felt that the method is sufficiently well illustrated by the circular tube case.

Important contributions to the analysis of laminar stratified flows in circular tubes have been made by Gemmell and Epstein (*1*) and by Charles and Redberger (*3*). In the absence of a practically viable analytical solution method, these authors employed numerical finite-differ-

ence techniques. Owing to an immediate interest in clarifying existing data for oil-water pipeline flows, results were obtained primarily for interfaces situated in the lower portion of the tube cross section. The results of references *1* and *3* will be compared with those of this investigation in a later section of the paper. It is also worthy of note that the aforementioned papers contain excellent summaries and interpretations of the experimental literature, exclusive of the recent study described in reference *2*. We have been unable to unearth experiments additional to those already discussed in these references.

Mathematically oriented studies aimed at formulating analytical solutions for the problem of stratified laminar flow are described by Dumitrescu and Stanescu (*4*) and by Bentwich (*5*). While these authors succeeded in devising approaches which provide solutions in principle, it remains a formidable task to use these methods to obtain results of practical interest, especially for ducts of arbitrary shape. For instance, in reference *5*, velocity distributions, expressed in terms of coordinates in a transformed complex plane, are stated as infinitely extended integrals. Although these analyses are very interesting from the mathematical viewpoint, it would appear that they are not highly promising from the standpoint of practical computation.

GENERAL ANALYTICAL FORMULATION

The physical model employed in the analysis will now be discussed. Consideration is extended to the fully developed, stably stratified flow of two immiscible fluids in a horizontal duct. The heavier fluid occupies the lower part of the duct cross section and the lighter fluid occupies the upper part. Each of the component fluids is assumed to be Newtonian, and laminar conditions prevail. The interface between the component flows is taken to be smooth and ripple free. Further, it is assumed that the interface is horizontal, that is, that the effects of preferential wetting of the duct wall are negligible. These same assumptions have served as the basis of the analyses reported in references *1* to *4*.

The recent carefully executed experimental study of Charles and Lilleleht (*2*) has lent support to this model. By employing visualization techniques, they demonstrated that laminar stratified flow (that is, laminar in both components) with a smooth, ripple-free interface is physically realizable. Excellent quantitative agreement between analysis and experiment was also found to exist. Each of the flow components (oil and water) of the experiment is Newtonian, and the aforementioned good agreement suggests that their Newtonian character is not altered when they interact in a stratified flow system.

Charles and Lilleleht observed a curving of the interface in the immediate neighborhood of the duct walls, but concluded that this is not an effect of first importance except in ducts of small horizontal dimensions. In this connection, it is of interest to note that the present solution method is in no way restricted to the case of a plane interface. Indeed, as will be demonstrated later, the position of the interface enters the solution method as a set of numerically specified coordinates, and it is of no consequence whether the coordinates describe a straight line or a curved line.

A schematic diagram of a stratified flow in a horizontal duct of arbitrary cross section is pictured at the left in Figure 1. The flow field is subdivided into two portions such that fluid 1 occupies the upper part of the duct and fluid 2 occupies the lower part. The cross-sectional coordinates are x, y, while the axial coordinate is z. In addition, the upper part of the duct wall is denoted by $C1$, the lower part of the wall by $C2$, and the interface by $C12$.

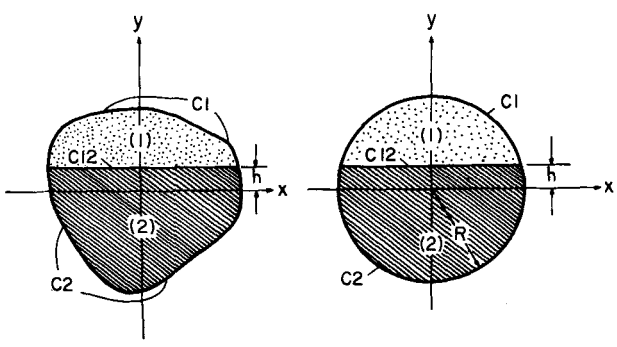

Fig. 1. Schematic diagrams of stratified flow in ducts.

The Governing Equations and Their Solution

The velocity field within each of the flow components is governed by the axial momentum equation, that is

$$\frac{\partial^2 u_i}{\partial x^2} + \frac{\partial^2 u_i}{\partial y^2} = \frac{1}{\mu_i}\frac{dP}{dz} = \text{const.}, \quad i = 1, 2 \qquad (1)$$

To facilitate the forthcoming development, the latter is transformed to Laplace's equation by introducing a reduced velocity u^*

$$u_i \Big/ \left(-\frac{L^2}{\mu_i}\frac{dP}{dz}\right) = u_i^* - \frac{1}{4}(x^2 + y^2), \quad i = 1, 2 \qquad (2)$$

where x and y are now dimensionless coordinates relative to a reference length L. It is readily verified that

$$\frac{\partial^2 u_i^*}{\partial x^2} + \frac{\partial^2 u_i^*}{\partial y^2} = 0, \quad i = 1, 2 \qquad (3)$$

Inasmuch as the velocity u is zero on the duct walls, it follows that the boundary values for u^* are

$$u_i^* = \frac{1}{4}(x_{ci}^2 + y_{ci}^2), \quad i = 1, 2 \qquad (4)$$

in which x_{ci} and y_{ci} denote the coordinates of boundary points. In addition, the velocity field must satisfy certain conditions of continuity at the interface. In particular, the velocities u_1 and u_2 must be equal at each point along the interfacial line and furthermore, there must be no net force. For a flat interface, this latter condition is expressible as $\mu_1\, \partial u_1/\partial y = \mu_2\, \partial u_2/\partial y$. When the continuity conditions are rephrased in terms of the transformed variables, one finds

$$\left.\begin{aligned} u_1^* - \left(\frac{\mu_1}{\mu_2}\right) u_2^* &= \frac{1}{4}(x^2 + y^2)\left(1 - \frac{\mu_1}{\mu_2}\right) \qquad (5a) \\ \frac{\partial u_1^*}{\partial y} &= \frac{\partial u_2^*}{\partial y} \qquad (5b) \end{aligned}\right\} \text{ on } C12$$

In order to determine the flow field, the pair of partial differential equations embodied in Equation (3) (Laplace's equation) must be solved subject to the boundary and interface conditions, Equations (4) and (5). As a first step in the solution, it is convenient to assemble a fundamental set of solutions of Laplace's equation. One systematic way of generating such solutions is by consideration of the real and imaginary parts of the complex variable $(x + y\sqrt{-1})^n$. For any non-negative integer n, the real and imaginary parts of the aforementioned complex variable are each solutions of Laplace's equation. Thus, by assigning to n the values 0, 1, 2, . . , as many

solutions as are desired can be obtained. The first seventeen of such solutions are listed in the Appendix where they are successively designated as $g_1, g_2, \ldots$.

With the g_j now available, the solutions for the reduced velocities u_1^* and u_2^* may be written as

$$u_1^* = \sum_{j=1}^{N_1} a_j g_j \qquad u_2^* = \sum_{j=1}^{N_2} b_j g_j \qquad (6)$$

The constants a_j and b_j remain to be determined, and for this purpose the boundary and interface conditions are available. Upon substituting Equations (6) into (4) and (5), there follows

$$\sum_{j=1}^{N_1} a_j g_j(x_{C1}, y_{C1}) = \frac{1}{4}(x^2_{C1} + y^2_{C1}) \qquad (7a)$$

$$\sum_{j=1}^{N_2} b_j g_j(x_{C2}, y_{C2}) = \frac{1}{4}(x^2_{C2} + y^2_{C2}) \qquad (7b)$$

$$\sum_{j=1}^{N_1} a_j g_j(x_{C12}, y_{C12}) - \left(\frac{\mu_1}{\mu_2}\right) \sum_{j=1}^{N_2} b_j g_j(x_{C12}, y_{C12}) = \frac{1}{4}(x^2_{C12} + y^2_{C12}) \left(1 - \frac{\mu_1}{\mu_2}\right) \qquad (7c)$$

$$\sum_{j=1}^{N_1} a_j \frac{\partial g_j}{\partial y}(x_{C12}, y_{C12}) - \sum_{j=1}^{N_2} b_j \frac{\partial g_j}{\partial y}(x_{C12}, y_{C12}) = 0 \qquad (7d)$$

It is interesting to note that the viscosities of the two flow components only enter the foregoing equations as a ratio μ_1/μ_2.

Now, suppose that Equation (7*a*) is imposed at each of n_1 points on the boundary $C1$, that Equation (7*b*) is imposed at each of n_2 points on $C2$, and that Equations (7*c*) and (7*d*) are imposed at each of n_{12} points on $C12$. Correspondingly, there are a total of $(n_1 + n_2 + 2n_{12}) = \tilde{n}$ linear algebraic equations. On the other hand, these equations contain $(N_1 + N_2) = \tilde{N}$ unknowns, that is, N_1 coefficients a_j and N_2 coefficients b_j. In general, to achieve a solution possessing the desired accuracy, $\tilde{n}$ will be much greater than $\tilde{N}$ (actual values will be discussed when the method is applied to the tube).

Under the conditions just discussed, the unknown constants a_j and b_j are readily determined by application of the least squares method, for which standard programs are available in the library of every modern electronic computer. There are several specific techniques by which the least squares procedure may be carried out. When dealing with large numbers of equations, it is especially advantageous to use the method of orthonormal functions, the basis for which is well described by Davis (6). The orthonormalization version of the least squares method is also available in the program libraries of modern computers.†

Thus, the values of the coefficients a_j and b_j are found without difficulty. Once these are available, the complete velocity solution follows in closed form from Equations (6) and (2).

It is interesting to observe that the flow field in all ducts of interest may be determined from a single computer program. The universal program would contain the algebraic expressions for the g_j and $\partial g_j/\partial y$, along with a statement of Equations (7*a*) through (7*d*). Then, to specialize to a particular duct configuration, it is only necessary to specify the points (x_{C1}, y_{C1}), (x_{C2}, y_{C2}), and (x_{C12}, y_{C12}), and the number of terms N_1 and N_2. Only this input information need be altered to accommodate successive duct configurations. It is also necessary to provide the ratio μ_1/μ_2 as input.

In applying the least squares method, it is necessary to specify weights for each of the participating equations. In the present application, a weight of unity was assigned to Equations (7*a*), while Equations (7*b*) through (7*d*) were weighted by a ratio of arc lengths. For this purpose, let Δs_1 denote the arc length between successive points on $C1$, and Δs_2 and Δs_{12} the corresponding arc lengths on $C2$ and $C12$. In terms of these quantities, Equation (7*b*) was weighted by the ratio $\Delta s_2/\Delta s_1$, while Equations (7*c*) and (7*d*) were weighted by $\Delta s_{12}/\Delta s_1$. In practice, the various arc lengths were selected so as to be as nearly identical as possible. Also, the number of terms N_1 and N_2 were chosen to be equal.

Representation of Velocity and Flow Results

Attention will now be directed to extracting various results of practical interest from the aforementioned solutions. First, the velocity field itself follows by combining Equations (6) and (2)

$$u_1 \Big/ \left(-\frac{L^2}{\mu_1}\frac{dP}{dz}\right) = \sum_{j=1}^{N_1} a_j g_j(x, y) - \frac{1}{4}(x^2 + y^2) \qquad (8a)$$

$$u_2 \Big/ \left(-\frac{L^2}{\mu_2}\frac{dP}{dz}\right) = \sum_{j=1}^{N_2} b_j g_j(x, y) - \frac{1}{4}(x^2 + y^2) \qquad (8b)$$

The volume flow rates Q_i for the respective components are found from

$$Q_i = \int_{A_i} u_i \, dA, \quad i = 1, 2 \qquad (9)$$

and the total flow rate Q is obtained by summing

$$Q = Q_1 + Q_2 \qquad (10)$$

Although the integration indicated in Equation (9) can in some cases be performed analytically, it is far more practical to carry out this task numerically within the computer. The integration required to determine Q_1 and Q_2 may be incorporated as part of the universal program that was discussed earlier.

There are several interesting representations of the volume-flow results. For instance, suppose that an apparent viscosity $\bar{\mu}$ of the two-component flow is defined by the relation

$$Q = K\left(-\frac{L^4}{\bar{\mu}}\frac{dP}{dz}\right) \qquad (11)$$

where K represents the numerical constant appropriate to the flow of a single homogeneous fluid through the given duct cross section. Then, upon combining Equations (9), (10), and (11), there follows

$$\frac{\bar{\mu}}{\mu_2} = K\left\{\int_{A_1} \frac{(\mu_2/\mu_1)\,u_1}{\left(-\frac{L^2}{\mu_1}\frac{dP}{dz}\right)} d\left(\frac{A}{L^2}\right) + \int_{A_2} \frac{u_2}{\left(-\frac{L^2}{\mu_2}\frac{dP}{dz}\right)} d\left(\frac{A}{L^2}\right)\right\}^{-1} \qquad (12)$$

Upon consideration of the foregoing in the light of Equations (8*a*) and (8*b*), and recalling that the a_j and b_j depend only on μ_1/μ_2 for a fixed-flow configuration, it follows that for each μ_1/μ_2 there is a corresponding $\bar{\mu}/\mu_2$. It

† For instance, for Control Data computers, the program is listed in the COOP library as E2 UOFM ORTHON.

TABLE 1. $\frac{Q_1^*}{Q_{1,\text{full}}}$ AND $1 - \frac{Q_2^*}{Q_{2,\text{full}}}$, CIRCULAR TUBE

$h/R \rightarrow$	−0.8	−0.6	−0.4	−0.2	0	0.2	0.4	0.6	0.8
Exact	0.98462	0.92281	0.81303	0.66639	0.50000	0.33361	0.18697	0.07719	0.01537
Present	0.98464	0.92282	0.81304	0.66640	0.50000	0.33361	0.18697	0.07719	0.01537

is evident that once $\bar{\mu}$ is known, the computation of the total flow rate Q from Equation (11) is a relatively straightforward operation.

One commonly employed measure of the effect of stratification on the volumetric flow rates of the separate components is the ratio

$$Q_i/Q_{i,\text{full}} \tag{13}$$

in which $Q_{i,\text{full}}$ represents the volume flow when fluid i fills the entire tube. The comparison of Q_i and $Q_{i,\text{full}}$ is made for the condition that the pressure gradients dP/dz are equal for the two situations. In analogy with Equation (11), $Q_{i,\text{full}}$ is expressible as

$$Q_{i,\text{full}} = K\left(-\frac{L^4}{\mu_i}\frac{dP}{dz}\right) \tag{14}$$

Then, for instance, for fluid 1, there follows from Equations (8a), (9), and (14)

$$\frac{Q_i}{Q_{i,\text{full}}} = \frac{1}{K}\int_{A_1}\left[\sum_{j=1}^{N_1} a_j g_j - \frac{1}{4}(x^2+y^2)\right] d\left(\frac{A}{L^2}\right) \tag{15}$$

and similarly for fluid 2. The ratio represented by Equation (15) depends parametrically on the flow configuration and on the viscosity ratio μ_1/μ_2.

When $Q_i/Q_{i,\text{full}}$ exceeds unity, a greater quantity of fluid i is transported by the stratified flow than by a full flow of i, under conditions of equal pressure gradient. Such a state of affairs is actually found to exist for the flow of highly viscous oils, with water added as the second flow component.

An alternate measure of the effect of stratification is to compare the pressure gradients dP/dz for a stratified flow and a full flow under the condition that $Q_i = Q_{i,\text{full}}$. For the flow component $i = 1$, it is readily verified that $(dP/dz)_{\text{full}}/(dP/dz)$ is numerically equal to the right-hand side of Equation (15), and similarly for fluid 2.

STRATIFIED FLOW IN A CIRCULAR TUBE

The application of the just described general formulation to flow in a circular tube will now be outlined and comparisons will be made with various limiting cases. Then, an exact solution is derived for the particular situation in which the interface coincides with the horizontal diameter of the tube. The presentation and discussion of results will be deferred until the last section of the paper.

Application of the General Formulation

The forthcoming discussion is facilitated by referring to the right-hand diagram of Figure 1. The origin of the x, y coordinate system is situated at the center of the circle. The vertical displacement of the interface from the x axis is represented by h, such that positive values of h indicate that the interface is above the x axis and negative values of h indicate that it is below the x axis.

In applying the general formulation, the reference length L is associated with the radius of the circle R. The essential step in determining the velocity field is to find the constants a_j and b_j by application of Equations (7). As a prelude to the least squares solution of this set of equations, h/R and μ_1/μ_2 are parametrically prescribed. Next, the numbers of terms, N_1 and N_2, are specified. Finally, the boundary points on $C1$ and $C2$ and the interface points on $C12$ at which the equations are to be evaluated are deduced by the computer according to instructions.

Solutions were carried out for nine values of h/R: 0, ± 0.2, ± 0.4, ± 0.6, and ± 0.8. At each position of the interface, μ_1/μ_2 was varied over the range from 1 to 1,000. For all interfacial positions except $h/R = \pm 0.8$, it was fully sufficient to take $N_1 = N_2 = 17$ and to use a total of 100 points on $C1$, $C2$, and $C12$. For $h/R = \pm 0.8$, a total of 250 points was employed. All solutions were carried out with the orthonormalization form of the least squares technique. Although the Control Data 1604 is by no means among the fastest computers, the running time for a typical case was about 1 min.

Owing to the symmetric placing of the axes, the constants a_j and b_j are zero for $j = 2, 5, 6, 9, 10, 13, 14$, and 17. A tabulation of the other constants for all of the cases investigated is extremely space-consuming and is therefore omitted. Such a tabulation is available from the authors on request.

With the a_j and b_j now available, all velocity and flow field results can be readily determined. Such results will be presented and discussed later. At this time, attention is directed to various comparisons that will aid in establishing the accuracy of the results.

In anticipation of the development presented in the next section, it may be noted that exact solutions for $u_1(x, y)$ and $u_2(x, y)$ corresponding to any μ_1/μ_2 can be obtained when $h/R = 0$. However, the integration required to determine the corresponding Q_1 and Q_2 cannot be performed analytically, and numerical means were employed. The Q_1 and Q_2 values corresponding to the exact solution are compared with those from the general calculation method developed earlier. In all cases, the agreement among the results is within 0.01% or better over the entire range from $\mu_1/\mu_2 = 1$ to 1,000! This finding is a clear testimony to the accuracies obtainable from the calculation method developed in this paper.

For the limiting case wherein $\mu_1/\mu_2 = 1$, exact results for Q_1 and Q_2 can be derived for any value of h/R. These are compared with the results from the present formulation in Table 1.† For purposes of future reference, the tabulated quantities are normalized by the corresponding values of Q_{full}. From an inspection of the table, it is clear that the two sets of results are in remarkably good agreement.

Another limiting case is encountered as $\mu_1/\mu_2 \rightarrow \infty$. This case, when viewed from the standpoint of fluid 2, corresponds to the condition in which fluid 1 is replaced by a rigid solid. In other words, fluid 2 is flowing in a duct of circular segment cross section. Exact solutions for fully developed laminar flow in circular segment ducts are not attainable; however, Sparrow and Haji-Sheikh (7) have obtained results that are believed to be accurate to well within 1%. These results are compared in Table 2 with those of the present investigation for $\mu_1/\mu_2 = 1{,}000$, which is the largest viscosity ratio considered here.

Inspection of the table reveals that when the interface lies in the upper portion of the duct ($h/R \geq 0$), the re-

† The asterisks appended to Q_1 and Q_2 will be explained later.

TABLE 2. VALUES OF $Q_2 \Big/ \left(-\frac{R^4}{\mu_2}\frac{dP}{dz}\right)$ FOR $\mu_1/\mu_2 = 1{,}000$ AND ∞

Circular tube

$h/R \rightarrow$	−0.8	−0.6	−0.4	−0.2	0	0.2	0.4	0.6	0.8
$\mu_1/\mu_2 = 1000$	0.000386	0.00390	0.01484	0.03798	0.07465	0.1279	0.1960	0.2723	0.3466
$\mu_1/\mu_2 = \infty$	0.000362	0.00383	0.01472	0.03720	0.07440	0.1275	0.1952	0.2720	0.3464

sults for $\mu_1/\mu_2 = 1{,}000$ and those for the circular segment duct are very nearly coincident, as they should be. However, as h/R becomes increasingly negative, greater deviations are observed. These trends are fully consistent with physical reasoning. Moreover, not only is this qualitative behavior reproduced by exact solutions for the square duct (obtained to facilitate the comparison) but also the percentage differences between the results for $\mu_1/\mu_2 = 1{,}000$ and $\mu_1/\mu_2 \rightarrow \infty$ are closely reproduced.

Upon reviewing the various comparisons with exact and with highly accurate limiting solutions, there appears to be ample evidence that the results provided by the present solution method are themselves of high accuracy.

Interface at $h/R = 0$

An exact solution for the case $h/R = 0$ can be attained with the aid of Green's functions. As a starting point, it is convenient to introduce a pair of reduced velocities $\hat{u}_1(x, y)$ and $\hat{u}_2(x, y)$ defined by

$$u_i = \hat{u}_i + \frac{dP/dz}{4\mu_i}(x^2 + y^2 - R^2), \quad i = 1, 2 \qquad (16)$$

in which x and y are dimensional coordinates. It is readily verified that both $\hat{u}_1$ and $\hat{u}_2$ satisfy Laplace's equation. Furthermore, the boundary and continuity conditions to be satisfied by the $\hat{u}_i$ take the form

$$\hat{u}_i = 0 \quad \text{on } C_i, \quad i = 1, 2 \qquad (17a)$$

$$\left.\begin{aligned} &\hat{u}_1(x, 0) - \hat{u}_2(x, 0) = -\frac{1}{4}\left(\frac{1}{\mu_1} - \frac{1}{\mu_2}\right)\frac{dP}{dz}(x^2 - R^2) \qquad (17b)\\ &\mu_1\frac{\partial \hat{u}_1}{\partial y} = \mu_2\frac{\partial \hat{u}_2}{\partial y} \qquad (17c)\end{aligned}\right\} \text{ on } C12$$

Now, let $\zeta = x + y\sqrt{-1}$ denote the complex coordinate of any point in the flow. Then, by employing the complex Green's function Γ (8), the value of $\hat{u}_i$ at ζ can be related to the boundary values by the relationship

$$\hat{u}_i(x, y) = -\Re\left\{\oint_c \hat{u}_i(x_c, y_c)\frac{d\Gamma}{dn}ds\right\}, \quad i = 1, 2 \qquad (18)$$

in which $\Re$ denotes the real part of the quantity in braces. The indicated integration extends over all parts of the contour that enclose the region i; for instance, if $i = 1$, then C is made up of $C1$ and $C12$. In the integrand, $\hat{u}_i(x_c, y_c)$ denotes the boundary values of $\hat{u}_i$, $d\Gamma/dn$ is the derivative of Γ with respect to the outer normal, and ds is the element of arc length.

Owing to the fact that $\hat{u}_i = 0$ on Ci, the integration need be carried out only on the diameter $C12$. Then, upon introducing $d\Gamma/dn$ appropriate to $C12$, there is obtained

$$\hat{u}_i(x, y) = -\Re\left\{\frac{(-1)^i\sqrt{-1}}{\pi}\int_{-R}^{R}\hat{u}_i(\lambda)\left[\frac{1}{\zeta - \lambda} - \frac{\zeta}{\zeta\lambda - R^2}\right]d\lambda\right\}, \quad i = 1, 2 \qquad (19)$$

in which λ is a dummy variable of integration. Next, after successively applying Equation (19) for $i = 1$ and $i = 2$ and then introducing the boundary conditions (17b) and (17c), there is obtained after considerable manipulation†

$$\int_{-R}^{R}\left[(\mu_1 + \mu_2)\frac{d\hat{u}_1(\lambda)}{d\lambda} + \frac{(\mu_2 - \mu_1)}{2\mu_1}\frac{dP}{dz}\lambda\right]\left(-\frac{1}{\lambda - x} - \frac{\lambda}{\lambda x - R^2}\right)d\lambda = 0 \qquad (20)$$

Since the integrand must be zero for any x, it follows that the first bracketed quantity is identically zero. This provides a first-order ordinary differential equation which can be solved for the interfacial velocity distribution $\hat{u}_1(x, 0) = \hat{u}_1(\lambda)$. A similar development yields $\hat{u}_2(x, 0)$. These quantities may be expressed as

$$\hat{u}_i(x, 0) = \frac{(-1)^{i+1}}{4\mu_i}\left(\frac{\mu_2 - \mu_1}{\mu_2 + \mu_1}\right)\frac{dP}{dz}(R^2 - x^2), \quad i = 1, 2 \qquad (21)$$

Furthermore, by employing Equation (16), there is obtained

$$u_1(x, 0) = u_2(x, 0) = -\frac{1/2}{(\mu_1 + \mu_2)}\frac{dP}{dz}(R^2 - x^2) \qquad (21a)$$

With the $\hat{u}_i$ along $C12$ now available from Equation (21), one may return to Equation (19) and perform the indicated integration in order to determine $\hat{u}_i(x, y)$. After a lengthy and involved development, there is derived

$$\hat{u}_i(x, y) = \frac{(-1)^i}{4\pi\mu_i}\left(\frac{\mu_1 - \mu_2}{\mu_1 + \mu_2}\right)\frac{dP}{dz}\left\{\pi\xi^2 + (-1)^i\left[R^2 + \xi^2 - \frac{R^2(x^2 - y^2)}{\rho^4}\right]\tan^{-1}\left(\frac{2Ry}{\xi}\right) + (-1)^i xy\left[1 - \frac{R^4}{\rho^4}\right]\right.$$

† Including integration by parts.

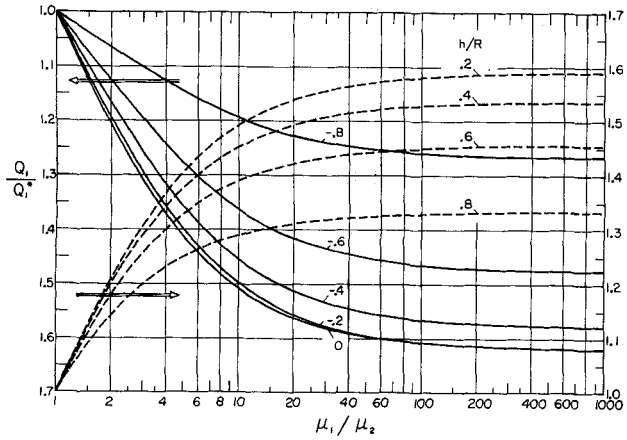

Fig. 2. Volumetric flow rate of fluid 1 (more viscous fluid) in a circular tube.

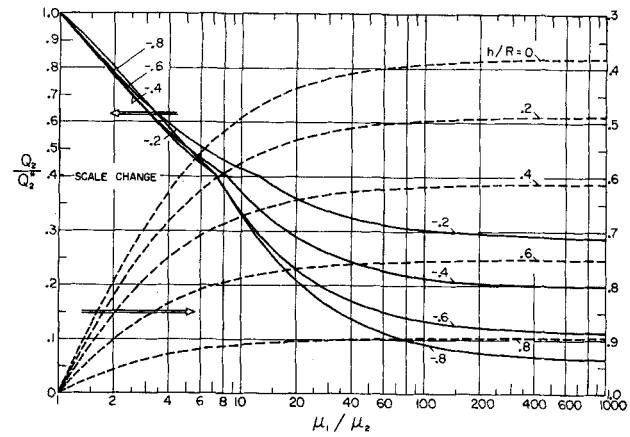

Fig. 3. Volumetric flow rate of fluid 2 (less viscous fluid) in a circular tube.

$$\ln \frac{(R-x)^2+y^2}{(R+x)^2+y^2} - (-1)^i \frac{2Ry\xi^2}{\rho^2} \Bigg\}, \quad i = 1, 2 \qquad (22)$$

where

$$\xi^2 = R^2 - x^2 + y^2, \quad \rho^2 = x^2 + y^2 \qquad (22a)$$

Equation (22), when taken together with Equation (16), provides an exact closed-form solution for the velocity field in both the upper half ($i = 1$) and the lower half ($i = 2$) of the tube. These solutions may be employed to compute flow rate quantities in accordance with Equations (9) through (15). As already noted, the numerical results are indistinguishable from those obtained by applying the general computation method developed earlier. Therefore, there is no need for separate presentation and discussion of the results from the exact solution.

RESULTS AND DISCUSSION

The quantity of most direct practical interest is the volumetric flow rate and its relationship to the pressure drop. In constructing a presentation of these results, the authors sought plotting parameters which would facilitate the accurate reading of graphs over the entire range of viscosity ratios μ_1/μ_2 and interface locations h/R.† To this end, reference flow quantities Q_1^* and Q_2^* are introduced. Q_1^* is the rate of volume flow passing through the part of the duct cross section that lies above the line $y = h$ when the entire duct is filled with fluid 1. Similarly, Q_2^* is the volume flow rate passing below the line $y = h$ when fluid 2 occupies the entire duct. It is readily shown that

$$\frac{Q_1^*}{Q_{1,\,\text{full}}} = 1 - \frac{Q_2^*}{Q_{2,\,\text{full}}} = \frac{1}{2} - \frac{2}{3\pi} \left[\frac{h}{R} \left(1 - \frac{h^2}{R^2}\right)^{3/2} + \frac{3}{2} \frac{h}{R} \left(1 - \frac{h^2}{R^2}\right)^{1/2} + \frac{3}{2} \sin^{-1} \frac{h}{R} \right] \qquad (23)$$

Numerical values corresponding to Equation (23) are listed in Table 1. In addition

$$Q_{i,\,\text{full}} \Big/ \left(-\frac{R^4}{\mu_i} \frac{dP}{dz} \right) = \frac{\pi}{8}, \quad i = 1, 2 \qquad (23a)$$

Results for the volumetric flow rate are presented in Figures 2 and 3, respectively, for fluids 1 and 2. The corresponding ordinate variables are Q_1/Q_1^* and Q_2/Q_2^*. These quantities are plotted against the viscosity ratio μ_1/μ_2 for parametric values of the interface location. In accordance with the definition of Q^*, all curves have ordinate values of unity when $\mu_1/\mu_2 = 1$. In each of the figures, there are two sets of curves. Those sloping upward to the right correspond to $h/R > 0$ and are referred to the right-hand ordinate; those sloping downward to the right are for $h/R < 0$ and are referred to the left-hand ordinate.

The quantities Q_i/Q_i^* have definite physical meanings. For instance, Q_2/Q_2^* compares the volumetric flow rates of component 2 that pass through the part of the cross section below the line $y = h$ under two different conditions. One condition is that the remainder of the cross section be occupied by fluid 1, while the second condition is that the remainder of the cross section be occupied by fluid 2. The pressure gradients are the same in the two cases. Since $\mu_1/\mu_2 > 1$, it is apparent from physical reasoning that $Q_2 < Q_2^*$. Furthermore, as μ_1/μ_2 increases, Q_2 will decrease monotonically, finally reaching a limit that corresponds to fluid 1 being replaced by a rigid body. These intuitive trends are consistent with the numerical results presented in Figure 3. A similar discussion pertains to Figure 2, wherein $Q_1/Q_1^* \geq 1$ for all values of the parameters. From both figures, it is seen that the flow rate results are rather insensitive to further increases in viscosity ratio when $\mu_1/\mu_2 > 100$.

It is also of interest to compare Q_1 (corresponding to any $h/R > -1$ and $\mu_1/\mu_2 > 1$) with the quantity $Q_{1,\,\text{full}}$, which corresponds to the case in which fluid 1 fills the entire cross section. The comparison is made for the condition of equal pressure gradients. If one plots $Q_1/Q_{1,\,\text{full}}$ against h/R for a fixed value of μ_1/μ_2, it is found that the resulting curve has a maximum (*1, 3*).

The values of such maxima are listed in Table 3 along with the locations h/R at which they occur. The tabulated results indicate that a stratified laminar flow is capable of passing as much as 37% more of component 1 than is a homogeneous flow with the same pressure gradient. It is interesting to note that the maximum $Q_1/Q_{1,\,\text{full}}$ reported in reference *1* is about 5% *higher* than the present value, while that reported in reference 3 is about 5% *lower* than the present value. Further inspection of the table shows that the interface location corresponding to the maximum $Q_1/Q_{1,\,\text{full}}$ is in the lower part of the tube cross section and is insensitive to μ_1/μ_2.

Inasmuch as the interface location h/R would not usually be known in practice, it is of interest to demonstrate how Figures 2 and 3 are used to determine all results of

† The graphical presentations employed in prior investigations (*1, 3,*) were concerned primarily with providing information for Q_1 when $h < 0$.

TABLE 3. MAXIMA OF $Q_1/Q_{1,\text{full}}$ FOR THE CIRCULAR TUBE

μ_1/μ_2	$Q_1/Q_{1,\text{full}}$	$-h/R$
10	1.26	0.59
100	1.36	0.59
1,000	1.37	0.59

practical interest. Among the six quantities Q_1, Q_2, dP/dz, h/R, μ_1 and μ_2, four must be prescribed. Suppose, for purposes of discussion, that μ_1, μ_2, Q_1, and dP/dz are given, and that Q_2 is desired. One would begin by guessing h/R. With this and the known μ_1/μ_2, a value of Q_1/Q_1^* is read from the ordinate of Figure 2. Next, Q_1 is found by multiplying Q_1/Q_1^* by the value of Q_1^* from Equations (23)† and (23*a*). If this Q_1 is equal to that prescribed, then the guessed value of h/R is correct. If not, then another guess is made for h/R and the procedure repeated. Once h/R has been determined, then Q_2 is found directly from Figure 3 with the aid of Equations (23)† and (23*a*). Of course, if h/R were somehow known a priori, then the trial and error procedure would not be necessary.

A convenient approach to computing the total volumetric flow rate Q of both components is to employ the apparent viscosity concept in conjunction with Equation (11). For the circular tube, the constant K is $\pi/8$ when the radius R is employed as the characteristic length L. Values of the apparent viscosity $\bar{\mu}$, deduced from the volume flow results, are presented in Figure 4. The ratio $\bar{\mu}/\mu_2$ is plotted as a function of μ_1/μ_2 for parametric values of the interface location h/R. In general, $\bar{\mu}/\mu_2 < \mu_1/\mu_2$. As $h/R \to 1$, $\bar{\mu}/\mu_2 \to 1$; conversely, as $h/R \to -1$, $\bar{\mu}/\mu_2 \to \mu_1/\mu_2$.

Before concluding the discussion of the circular tube, it is appropriate to compare the present results with those of references *1* and *3*, wherein finite-difference methods were employed. Both of these investigations were concerned primarily with $h/R \leq 0$. Considering first reference *1*, the Q_1 results in the range $-1 \leq h/R \leq 0$ are typically within 5% of the present values; however, deviations in Q_2 of up to 15% are found to exist when h/R is close to -1. In the range $h/R > 0$, reference *1* reports a solution only for $h/R = 0.5$. There is some difficulty in achieving a precise reading from Figure 7 of the reference, but it is believed that there is agreeement with the present results to within 5%.

In reference *3*, results are given only for Q_1. For $h/R \leq 0$, the Q_1 values of this reference are within 5% of the present values, but the deviations are of opposite sign compared with those noted in connection with reference *1*. No indication is given as to which points were computed in reference *3* for $h/R > 0$. It appears that the graphically presented Q_1 results are in satisfactory agreement with the present ones for h/R up to 0.6, beyond which substantial deviations occur.

On the whole, the foregoing comparisons indicate a satisfactory level of agreement. However, it appears that there may be some difficulty in obtaining accurate values of Q_1 and Q_2 from a square-mesh, finite-difference grid, respectively, when h/R approaches 1 and -1.

† Or, alternatively, Table 1.

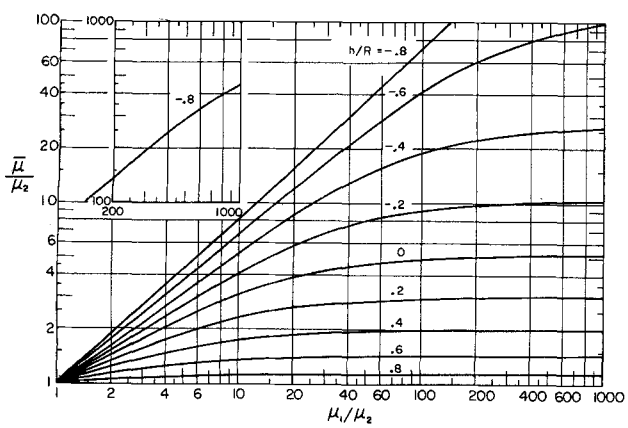

Fig. 4. Apparent viscosity for a two-component stratified laminar flow in a circular tube.

NOTATION

A = cross-sectional area
g_j = solutions of Laplace's equation, see Appendix
h = location of interface
L = characteristic length
Q_i = volumetric flow rate of component i
Q_1^* = value of Q_i for $\mu_1/\mu_2 = 1$
$Q_{i,\text{full}}$ = value of Q_i when component i fills duct
Q = overall flow rate, $(Q_1 + Q_2)$
P = static pressure
R = tube radius
u = axial velocity
u^*, $\hat{u}$ = reduced velocities
x, y = cross-sectional coordinates
z = axial coordinate
μ = viscosity
$\bar{\mu}$ = apparent viscosity

Subscripts

1 = more viscous fluid
2 = less viscous fluid

LITERATURE CITED

1. Gemmell, A. R., and Norman Epstein, *Can. J. Chem. Eng.*, **40**, 215 (1962).
2. Charles, M. E., and L. U. Lilleleht, *ibid.*, **43**, 110 (1965).
3. Charles, M. E., and P. J. Redberger, *ibid.*, **40**, 70 (1962).
4. Dumitrescu, L., and C. Stanescu, *Acad. Rep. Populare Romine, Rev. Mecan. Appl.*, **2**, 2 (1957).
5. Bentwich, M., *J. Basic Eng.*, **D86**, 669 (1964).
6. Davis, P. J., in "Survey of Numerical Analysis," J. Todd, ed., McGraw-Hill, New York (1962).
7. Sparrow, E. M., and A. Haji-Sheikh, *ASME paper 65-WA/HT-13*, to be published.
8. Jacob, C., "Introduction Mathematique à la Méchanique des Fluides," Gauthier-Villars, Paris (1959).

APPENDIX: THE *g* FUNCTIONS

$g_1 = 1$
$g_2 = x$
$g_3 = y$
$g_4 = x^2 - y^2$
$g_5 = 2xy$
$g_6 = x^3 - 3xy^2$
$g_7 = 3x^2y - y^3$
$g_8 = x^4 + y^4 - 6x^2y^2$
$g_9 = 4x^3y - 4xy^3$
$g_{10} = x^5 - 10x^3y^2 + 5xy^4$
$g_{11} = y^5 - 10y^3x^2 + 5yx^4$
$g_{12} = x^6 - 15x^4y^2 + 15x^2y^4 - y^6$
$g_{13} = 6x^5y + 6xy^5 - 20x^3y^3$
$g_{14} = x^7 - 21x^5y^2 + 35x^3y^4 - 7xy^6$
$g_{15} = 7x^6y - 35x^4y^3 + 21x^2y^5 - y^7$
$g_{16} = x^8 + y^8 - 28x^6y^2 + 70x^4y^4 - 28x^2y^6$
$g_{17} = 8x^7y - 56x^5y^3 + 56x^3y^5 - 8xy^7$

Manuscript received January 24, 1966; revision received May 11, 1966; paper accepted June 16, 1966.